

UC San Diego

UC San Diego Previously Published Works

Title

B decays to two pseudoscalars and a generalized $\Delta I=1/2$ rule

Permalink

<https://escholarship.org/uc/item/0bk1t0vd>

Journal

Physical Review D, 89(11)

ISSN

2470-0010

Authors

Grinstein, Benjamín
Stone, David C
Pirskhalava, David
[et al.](#)

Publication Date

2014-06-01

DOI

10.1103/physrevd.89.114014

Peer reviewed

B decays to two pseudoscalars and a generalized $\Delta I = \frac{1}{2}$ rule

Benjamín Grinstein* and David C. Stone†
*Department of Physics, University of California,
 San Diego, La Jolla, CA 92093 USA*

David Pirtskhalava‡
Scuola Normale Superiore, Piazza dei Cavalieri 7, 56126 Pisa, Italy

Patipan Uttayarat§
*Department of Physics, University of Cincinnati, Cincinnati, OH 45220 USA and
 Department of Physics, Srinakharinwirot University, Wattana, Bangkok 10110 Thailand*

Abstract

We perform an isospin analysis of B decays to two pseudoscalars. The analysis extracts appropriate CKM and short distance loop factors to allow for comparison of non-perturbative QCD effects in the reduced matrix elements of the amplitudes. In decays where penguin diagrams compete with tree-level diagrams we find that the reduced matrix elements of the penguin diagrams, which are singlets or doublets under isospin, are significantly enhanced compared with the triplet and fourplet contributions of the weak Hamiltonian. This similarity to the $\Delta I = \frac{1}{2}$ rule in $K \rightarrow \pi\pi$ decays suggests that, more generally, processes mediated by Hamiltonians in lower-dimensional isospin representations see enhancement over higher-dimensional ones in QCD.

I. INTRODUCTION

One of the longstanding puzzles in flavor physics is the $\Delta I = 1/2$ rule. An isospin- $\frac{1}{2}$ neutral kaon may decay into two pions in either an isospin-0 or isospin-2 (s -wave) state with amplitude A_0 or A_2 , respectively. Empirically,

$$\frac{\text{Re } A_0}{\text{Re } A_2} = 22.5 . \quad (1)$$

The $\Delta I = 1/2$ rule is the statement that the amplitude A_0 , mediated by the part of the weak Hamiltonian that transforms as an $I = 1/2$ tensor, is much larger than A_2 , mediated by the larger $I = 3/2$ tensor.

There is no satisfactory understanding of this rule. In Refs. [1–3] and, more recently, Ref. [4] the rule was investigated in chiral perturbation theory, in the large N_c limit. However, it was argued in Ref. [5] that for QCD, $N_c = 3$ is not large enough for this limit to be useful. More recent studies using Monte Carlo simulations of QCD in the lattice have addressed the $\Delta I = 1/2$ rule [6]; a very recent study on the lattice of the validity of the vacuum insertion approximation was done in [7]. The ratio in (1) is still twice as large as any values obtained on the lattice with unphysical quark masses, but it is expected that simulations at physical quark masses will reproduce the empirically observed ratio and shed light on the origin of the enhancement [8]. This begs the question— does this enhancement occur in systems other than the $K \rightarrow \pi\pi$ system?

There is evidence that answers this question in the affirmative. Identifying any patterns of

* bgrinstein@ucsd.edu

† dcstone@physics.ucsd.edu

‡ david.pirtskhalava@sns.it

§ uttayapn@ucmail.uc.edu

enhancements will give new insights into the long distance dynamics of QCD. For example, the $SU(3)$ analysis of $D \rightarrow KK, \pi\pi$ decays reveals a similar enhancement. In that system, the $D^0 \rightarrow K^+K^-$ and $D^0 \rightarrow \pi^+\pi^-$ amplitudes may be written as [9]

$$\begin{aligned}\mathcal{A}(D^0 \rightarrow K^+K^-) &= (2T + E - S)\Sigma \\ &\quad + \frac{1}{2}(3T + 2G + F - E)\Delta \\ \mathcal{A}(D^0 \rightarrow \pi^+\pi^-) &= -(2T + E - S)\Sigma \\ &\quad + \frac{1}{2}(3T + 2G + F - E)\Delta\end{aligned}$$

where $\Sigma \equiv \frac{1}{2}(V_{cs}^*V_{us} - V_{cd}^*V_{ud})$ and $\Delta \equiv \frac{1}{2}(V_{cs}^*V_{us} + V_{cd}^*V_{ud})$. S , E and F are the invariant matrix elements between a D meson and a meson pair in an octet of the $\bar{\mathbf{6}}$, $\mathbf{15}$ and $\mathbf{3}$ components of the weak Hamiltonian, respectively, G of the $\mathbf{3}$ to a singlet pair and T of the $\mathbf{15}$ to a meson pair in the $\mathbf{27}$. Note that $\Sigma \approx \lambda = \sin\theta_C$, while $|\Delta| \sim \lambda^5$, so that $|\Delta|/\Sigma \sim 10^{-3}$. Neglecting Δ one would have $\Gamma(D^0 \rightarrow K^+K^-) = \Gamma(D^0 \rightarrow \pi^+\pi^-)$ in the $SU(3)$ limit. Experimentally $\Gamma(D^0 \rightarrow K^+K^-)/\Gamma(D^0 \rightarrow \pi^+\pi^-) \approx 3$ requires both the Σ and Δ terms in the amplitude to contribute with similar strengths. Barring accidental cancellations this means that the matrix elements G and F are significantly enhanced. Since Δ has a large phase, significant CP-violation in these decays was predicted [10] and recently confirmed by experiment [11–13].

If $SU(3)$ -breaking effects are included, the ratio $\Gamma(D^0 \rightarrow K^+K^-)/\Gamma(D^0 \rightarrow \pi^+\pi^-) \approx 3$ can be attained with only a “mild” enhancement of F and G relative to the other reduced matrix elements of about an order of magnitude [14–19]. The enhancement in F and G is similar to that of the $\Delta I = 1/2$ rule in that it appears in matrix elements of the smallest $SU(3)$ -representation of the Hamiltonian. In this case, the dominant contributions are from the $\mathbf{3}$ Hamiltonian (as opposed to the $\bar{\mathbf{6}}$ and $\mathbf{15}$), whereas for the $\Delta I = 1/2$ rule the dominant piece is from the $I = 1/2$ Hamiltonian (as opposed to the $I = 3/2$

piece).

In this work we investigate the possibility of similar enhancements in B decays. We will show that an isospin analysis of $B \rightarrow K\pi$ decays and CP-asymmetries shows a marked enhancement of amplitudes mediated by the weak Hamiltonian in the lowest isospin representation. An analysis of $B \rightarrow \pi\pi$ decays shows that, although there is little enhancement of doublet versus fourplet amplitudes, the matrix elements of penguin contributions (which are purely $\Delta I = 1/2$) are still enhanced to produce the observed data. Both these analyses support the general rule that amplitudes mediated by the piece of the weak Hamiltonian in the smallest representation of the symmetry group are enhanced.

It should go without saying that we have no dynamical explanation of the enhancement. This comes as no surprise, since the very $\Delta I = 1/2$ rule has resisted explanation for more than a half century. But we hope that insights provided by this new, generalized rule may eventually lead to a global understanding of these enhancements.

II. ISOSPIN ANALYSIS

The strong interactions, to a good approximation, obey isospin symmetry. In hadronic spectra and decays isospin violating effects are no larger than a few per cent. We study the amplitudes for the decay of B -mesons to two light scalar mesons using isospin symmetry, under which kaons and B -mesons transform as doublets and pions as a triplet. The possible two-body final states are easily classified according to their transformation properties under isospin. We also need the transformation properties of the effective Hamiltonian responsible for the weak decay. The effective Hamiltonian is given in terms of four-quark operators, whose transformation properties are readily de-

terminated.

A. $B \rightarrow K\pi$

The effective Hamiltonian density for the $\Delta B = -1$, $\Delta S = -1$ decays, to leading order in the Fermi constant G_F , can be written as [20, 21]

$$\mathcal{H} = \frac{G_F}{\sqrt{2}} \left[\lambda_u (C_1 Q_1 + C_2 Q_2) - \lambda_t \sum_{i=3}^6 C_i Q_i \right]. \quad (2)$$

Here $\lambda_q \equiv V_{qb}^* V_{qs}$ are CKM factors and C_i 's are the Wilson coefficients. The ‘‘tree’’ ($Q_{1,2}$) and ‘‘penguin’’ (Q_{3-6}) operators are defined as

$$\begin{aligned} Q_1 &= (\bar{b}_a u_b)_{V-A} (\bar{u}_b s_a)_{V-A}, \\ Q_2 &= (\bar{b}u)_{V-A} (\bar{u}s)_{V-A}, \\ Q_3 &= (\bar{b}s)_{V-A} \sum_{q=u,d} (\bar{q}q)_{V-A}, \\ Q_4 &= (\bar{b}_a s_b)_{V-A} \sum_{q=u,d} (\bar{q}_b q_a)_{V-A}, \\ Q_5 &= (\bar{b}s)_{V-A} \sum_{q=u,d} (\bar{q}q)_{V+A}, \\ Q_6 &= (\bar{b}_a s_b)_{V-A} \sum_{q=u,d} (\bar{q}_b q_a)_{V+A} \end{aligned} \quad (3)$$

where $(\bar{q}q)_{V\pm A}$ is shorthand for $\bar{q}\gamma^\mu(1 \pm \gamma^5)q$. Both the coefficients C_i and the matrix elements of the operators Q_i depend on an arbitrary renormalization point μ but their combination in the Hamiltonian, Eq. (2), is μ -independent. QCD-penguins arising from u and c quark loops combine into terms precisely of the form of top-quark penguins, since $\lambda_c + \lambda_u = -\lambda_t$. We have also neglected electroweak penguins (EWP), operators Q_{7-10} in Ref. [20]. These introduce new isospin triplets into the Hamiltonian with a λ_t coefficient, suppressed relative to the top-penguins by α/α_s . We have ignored EWP contributions out of pragmatism: were we to include their effects in our fits the number of un-

known matrix elements would exceed the number of measured data. But our pragmatism is informed: the coefficients of EWP in the effective Hamiltonian are suppressed relative to QCD penguins roughly by a factor of α/α_s , or about 7% if evaluated at $\mu = M_Z$ and smaller at m_b . As will become evident, the approximation is supported by the very good fit of the model to both $B \rightarrow K\pi$ and $B \rightarrow \pi\pi$ processes.

As far as the group theory analysis of rates and CP asymmetries is concerned, different four-quark operators contributing to the Hamiltonian can be distinguished solely by their isospin quantum numbers and CKM factors. The Hamiltonian can therefore be compactly written in terms of the isospin representations in the following way:

$$H = V_{ub}^* V_{us} (\mathbf{1} + [\mathbf{3}]^1_1) + \frac{\alpha_s}{8\pi} V_{tb}^* V_{ts} \mathbf{1}', \quad (4)$$

where $\mathbf{1}$ ($\mathbf{1}'$) denotes the singlet coming from the tree (penguin) operators, $[\mathbf{3}]^1_1$ represents the triplet operator, and α_s the strong coupling constant evaluated at M_Z . We choose to normalize the singlet penguin operator with an agnostic factor of $\alpha_s/(8\pi)$ to make explicit the loop factor associated with it. This normalization does not affect the results of this paper, but it is a useful choice that, naively, would give reduced matrix element values of the same order of magnitude for every contribution. We introduce shorthand for the reduced matrix elements, as follows:

$$\begin{aligned} \langle \bar{\mathbf{2}}|\mathbf{1}|B \rangle &\equiv P_b, & \langle \bar{\mathbf{2}}|\mathbf{1}'|B \rangle &\equiv P_a, \\ \langle \bar{\mathbf{2}}|\mathbf{3}|B \rangle &\equiv T, & \langle \bar{\mathbf{4}}|\mathbf{3}|B \rangle &\equiv S. \end{aligned} \quad (5)$$

While we cannot compute P_a , P_b , S and T from first principles, we can determine them by fitting to experimental measurements of decay rates and CP asymmetries.

In terms of the reduced matrix elements in Eq. (5), the isospin decomposition of the decay

Mode	\mathcal{B} (10^{-6})	A_{CP}	C_f	S_f
$B^+ \rightarrow K^+\pi^0$	12.9 ± 0.5	0.037 ± 0.021	–	–
$B^+ \rightarrow K^0\pi^+$	23.8 ± 0.7	-0.014 ± 0.019	–	–
$B_d^0 \rightarrow K^0\pi^0$	9.9 ± 0.5	–	0.00 ± 0.13	0.58 ± 0.17
$B_d^0 \rightarrow K^+\pi^-$	19.6 ± 0.5	-0.087 ± 0.008	–	–

TABLE I: Data available in $B \rightarrow K\pi$ decays [22]. The C and S parameters are measured for decays into the final CP eigenstate, $B_d^0 \rightarrow K_s^0\pi_0$. The amplitude for $B_d^0 \rightarrow K^0\pi^0$ on the other hand is given as $\mathcal{A}(B_d^0 \rightarrow K^0\pi^0) = \sqrt{2} \mathcal{A}(B_d^0 \rightarrow K_s^0\pi^0)$.

amplitudes is

$$\begin{aligned}
\mathcal{A}(B^+ \rightarrow K^+\pi^0) &= V_{ub}^* V_{us} \frac{1}{\sqrt{2}} (P_b + T + 2S) \\
&\quad + \frac{\alpha_s}{8\pi} V_{tb}^* V_{ts} \frac{P_a}{\sqrt{2}}, \\
\mathcal{A}(B^+ \rightarrow K^0\pi^+) &= V_{ub}^* V_{us} (P_b + T - S) \\
&\quad + \frac{\alpha_s}{8\pi} V_{tb}^* V_{ts} P_a, \\
\mathcal{A}(B^0 \rightarrow K^0\pi^0) &= V_{ub}^* V_{us} \frac{1}{\sqrt{2}} (-P_b + T + 2S) \\
&\quad - \frac{\alpha_s}{8\pi} V_{tb}^* V_{ts} \frac{P_a}{\sqrt{2}}, \\
\mathcal{A}(B^0 \rightarrow K^+\pi^-) &= V_{ub}^* V_{us} (P_b - T + S) \\
&\quad + \frac{\alpha_s}{8\pi} V_{tb}^* V_{ts} P_a. \tag{6}
\end{aligned}$$

There is a contribution proportional to $V_{ub}^* V_{us}$ to the amplitude $\mathcal{A}(B^+ \rightarrow K^0\pi^+)$. The only contribution to this process stems from the annihilation diagram, shown in Fig. 1. There is extensive literature on annihilation diagram suppression with respect to W -emission diagrams [23, 24]. To evaluate this expectation, denote the matrix element associated with the annihilation diagram by $M \equiv P_b + T - S$ and let $|M| = x|P_a|$ so that x measures the relative importance of annihilation in comparison to the top-loop penguin. The value of x for which the annihilation and penguin contributions to $B^+ \rightarrow K^0\pi^+$ are of the same order can be estimated as

$$x = \frac{\alpha_s}{8\pi} \left| \frac{V_{tb}^* V_{ts}}{V_{ub}^* V_{us}} \right| \simeq 0.24. \tag{7}$$

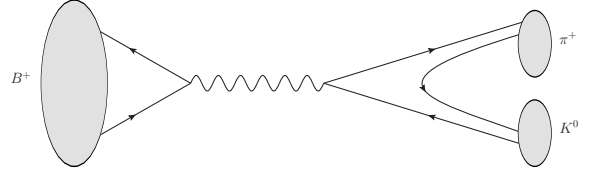


FIG. 1: Leading order diagram contributing to the $B^+ \rightarrow K^0\pi^+$ process.

Results of the fit

The available decay data for $B \rightarrow K\pi$ are collected in Table I; the observables are defined in Appendix A. Performing a χ^2 fit of matrix elements in Eq. (6) to the data, we find values for the matrix elements that match the observed data with a 95% confidence level. These minima are illustrated with 68% and 95% confidence levels in the $|P_a|$ vs. $|P_b|$ and $|P_a|$ vs. $|T|$ planes, respectively, in Fig. 2. The best fit has $\{|P_a|, |P_b|, |T|, |S|\} \simeq \{0.237, 7.2 \times 10^{-3}, 8.4 \times 10^{-3}, 2.2 \times 10^{-3}\}$ MeV with a chi-squared of $\chi^2 = 1.70$ for two degrees of freedom (a common phase in the reduced matrix elements is unobservable). The $\Delta I = 0$ contribution to the amplitudes, from the Hamiltonian in the singlet representation, is given by the quantity

$$a_{\Delta I=0} = P_b + \frac{\alpha_s}{8\pi} \frac{V_{tb}^* V_{ts}}{V_{ub}^* V_{us}} P_a \tag{8}$$

and the $\Delta I = 1$ contribution, from the triplet Hamiltonian, by

$$a_{\Delta I=1} = \{T + 2S, T - S\}. \tag{9}$$

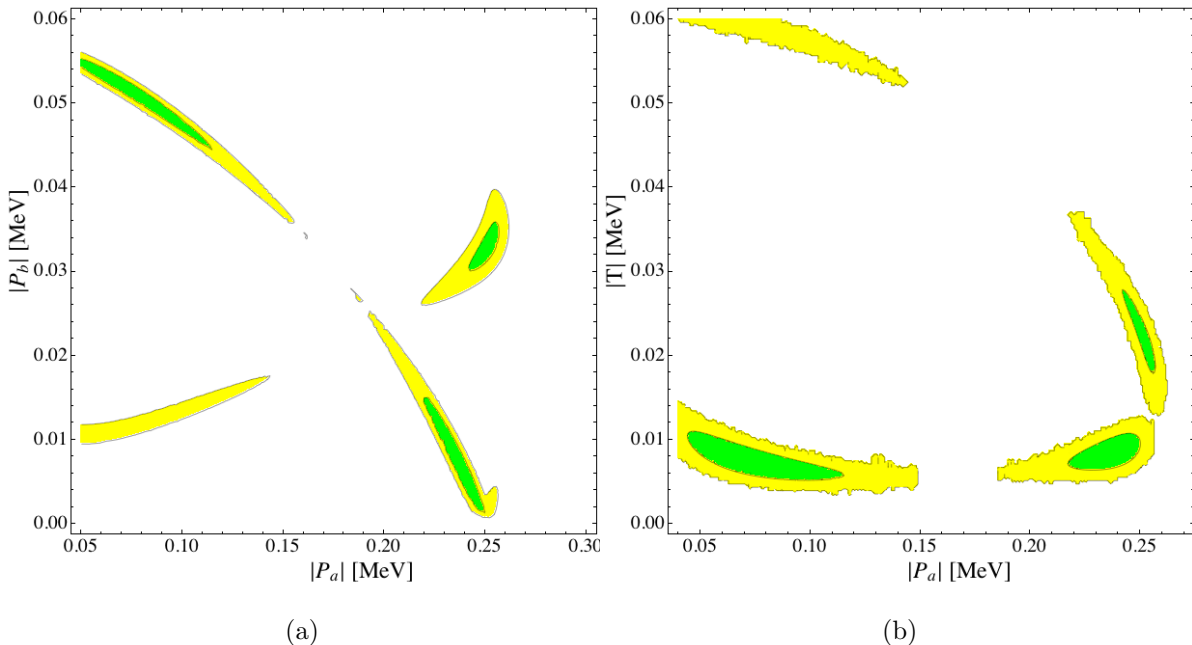


FIG. 2: Fit to data of the reduced matrix elements for $B \rightarrow K\pi$. The figures show the 68% (green) and 95% (yellow) CL regions in the $|P_a|$ vs $|P_b|$ and $|P_a|$ vs $|T|$ planes. The raggedness of the contours is an artifact of the numerical computation.

for $(B^+ \rightarrow K^+\pi^0, B^0 \rightarrow K^0\pi^+)$ and $(B^+ \rightarrow K^0\pi^+, B^0 \rightarrow K^+\pi^-)$ respectively. For the best fit then, we find

$$\left| \frac{a_{\Delta I=0}}{a_{\Delta I=1}} \right| = \{4.8, 9.9\} \quad (10)$$

which is reminiscent of the $\Delta I = \frac{1}{2}$ rule from $K \rightarrow \pi\pi$ decays.

A second, slightly higher χ^2 -minimum has $\{|P_a|, |P_b|, |T|, |S|\} \simeq \{0.075, 0.052, 7.3 \times 10^{-3}, 2.4 \times 10^{-3}\}$ MeV with a chi-squared of $\chi^2 = 1.80$ and

$$\left| \frac{a_{\Delta I=0}}{a_{\Delta I=1}} \right| = \{5.2, 12.6\}. \quad (11)$$

Both of these minima have significant enhancement of the *penguin* singlet, P_a , over the triplet matrix elements, T and S . In the best fit case, however, the other singlet matrix element, P_b , does not show significant enhancement over the triplet matrix elements. Consequently, the

annihilation diagram contribution is negligible in the best fit ($|M| = 0.013$ MeV or, equivalently, $x = |M/P_a| = 0.055$, to be compared with Eq. (7)) but provides a larger contribution than that of the penguin diagram in the second best fit (where $|M| = 0.055$ MeV or, equivalently, $x = 0.732$).

For completeness we note that there are two additional minima corresponding to $\chi^2 = 3.04$ and 4.34. These two minima are less favorable, so we ignore them in the rest of our study.

In all but the least favored minimum, there is significant enhancement of $|P_a|$ over the triplet Hamiltonian matrix elements. Moreover, the total contribution from the $\Delta I = 0$ Hamiltonian, $a_{\Delta I=0}$, enjoys an enhancement over the $\Delta I = 1$ contribution, $a_{\Delta I=1}$. More precise data will be welcomed to distinguish between these minima, which would also decide the role of the annihilation diagram in these decays.

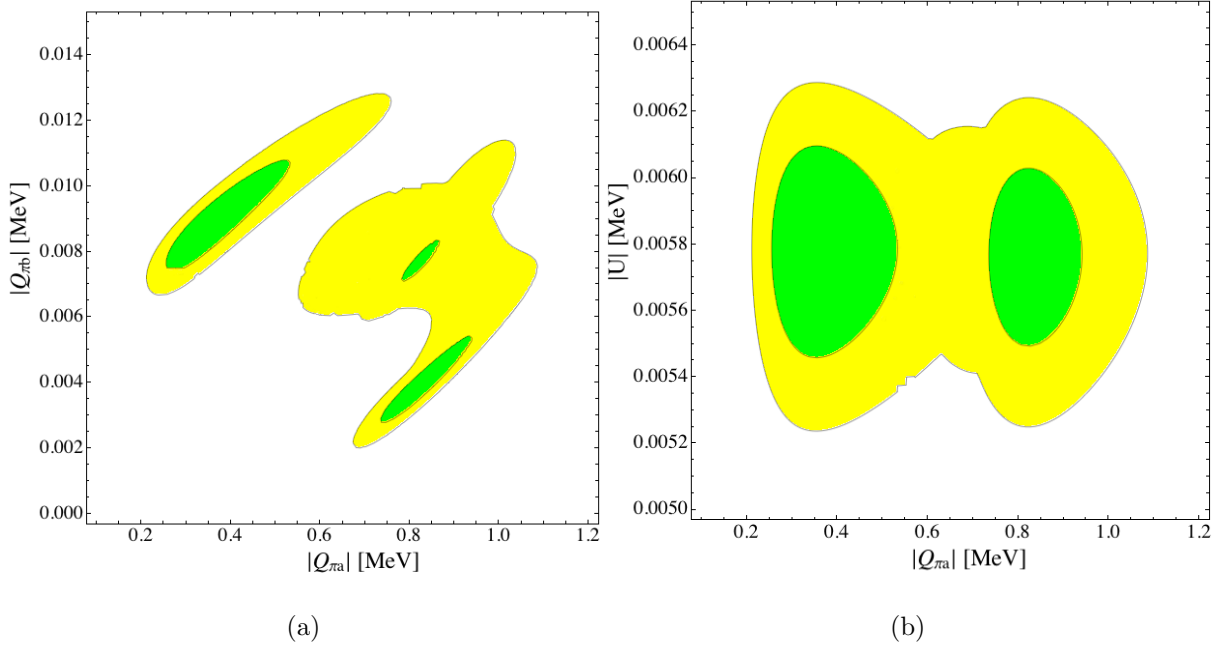


FIG. 3: Fit to data of the reduced matrix elements for $B \rightarrow \pi\pi$. The figures show the 68% (green) and 95% (yellow) CL regions in the $|Q_{\pi a}|$ vs $|Q_{\pi b}|$ and $|Q_{\pi a}|$ vs $|U|$ planes. The raggedness of the contours is an artifact of the numerical computation.

B. $B \rightarrow \pi\pi$

The isospin analysis for $\pi\pi$ final states is analogous to that for K decays, where the $\Delta I = \frac{1}{2}$ rule was discovered. Operator contributions are of the form in (3), but for $\Delta S = 0$ processes. The Hamiltonian decomposes under isospin as $\bar{\mathbf{2}} \times \mathbf{2} \times \bar{\mathbf{2}} = \bar{\mathbf{2}} + \bar{\mathbf{2}} + \bar{\mathbf{4}}$ so that

$$H = V_{ub}^* V_{ud} \left([\bar{\mathbf{2}}]^2 + [\bar{\mathbf{4}}]_1^{12} \right) + \frac{\alpha_s}{8\pi} V_{tb}^* V_{ts} [\bar{\mathbf{2}}']^2, \quad (12)$$

The final states transform as $(\mathbf{3} \times \mathbf{3})_S = \mathbf{1} + \mathbf{5}$, so the non-vanishing reduced matrix elements are

$$\langle \mathbf{1} | \bar{\mathbf{2}}' | B \rangle = Q_{\pi a}, \quad \langle \mathbf{1} | \bar{\mathbf{2}} | B \rangle = Q_{\pi b}, \quad \langle \mathbf{5} | \bar{\mathbf{4}} | B \rangle = U \quad (13)$$

and the decay amplitudes relevant to the processes in Table II are

$$\begin{aligned} \mathcal{A}(B^+ \rightarrow \pi^+ \pi^0) &= \sqrt{\frac{3}{2}} V_{ub}^* V_{ud} U, \\ \mathcal{A}(B^0 \rightarrow \pi^0 \pi^0) &= V_{ub}^* V_{ud} \frac{1}{\sqrt{3}} \left(Q_{\pi b} - \sqrt{2} U \right) \end{aligned}$$

$$\begin{aligned} &+ \frac{\alpha_s}{8\pi} V_{tb}^* V_{td} \frac{1}{\sqrt{3}} Q_{\pi a}, \\ \mathcal{A}(B^0 \rightarrow \pi^+ \pi^-) &= V_{ub}^* V_{ud} \frac{1}{\sqrt{3}} \left(\sqrt{2} Q_{\pi b} + U \right) \\ &+ \frac{\alpha_s}{8\pi} V_{tb}^* V_{td} \sqrt{\frac{2}{3}} Q_{\pi a}. \end{aligned} \quad (14)$$

Results of the fit

The data available in this decay channel are listed in Table II. We perform a χ^2 -fit of the model, Eq. (14), to the data. The result of the fit is illustrated with 68% (green) and 95% (yellow) CL regions in the $|Q_{\pi a}|$ vs $|Q_{\pi b}|$ and $|Q_{\pi a}|$ vs $|U|$ planes, respectively, in Fig. 3. For the best fit to the data we obtain $\{|Q_{\pi a}|, |Q_{\pi b}|, |U|\} \simeq \{0.35, 8.8 \times 10^{-3}, 5.8 \times 10^{-3}\}$ MeV with a chi-squared of $\chi^2 \simeq 1.39$ for 2 degrees of freedom. Two additional regions with a good fit to the data are found, one with $\{|Q_{\pi a}|, |Q_{\pi b}|, |U|\} \simeq$

Mode	\mathcal{B} (10^{-6})	A_{CP}	C_f	S_f
$B^+ \rightarrow \pi^+\pi^0$	5.5 ± 0.4	0.03 ± 0.04	–	–
$B^0 \rightarrow \pi^0\pi^0$	1.91 ± 0.22	–	-0.43 ± 0.24	–
$B^0 \rightarrow \pi^+\pi^-$	5.12 ± 0.19	–	-0.38 ± 0.15	-0.65 ± 0.07

TABLE II: Data available in $B \rightarrow \pi\pi$ decays from Ref [22].

$\{0.82, 3.9 \times 10^{-3}, 5.8 \times 10^{-3}\}$ MeV for a chi-squared of $\chi^2 \simeq 2.07$ and the other with $\{|Q_{\pi a}|, |Q_{\pi b}|, |U|\} \simeq \{0.82, 7.7 \times 10^{-3}, 5.8 \times 10^{-3}\}$ MeV for a chi-squared of $\chi^2 \simeq 3.38$. Since the last minimum is less favorable, we will ignore it. The contribution to the amplitudes from the Hamiltonian in the doublet representation is

$$a_{\Delta I=1/2} = Q_{\pi b} + \frac{\alpha_s}{8\pi} \frac{V_{tb}^* V_{td}}{V_{ub}^* V_{ud}} Q_{\pi a} \quad (15)$$

and from the fourplet Hamiltonian

$$a_{\Delta I=3/2} = U. \quad (16)$$

We find no enhancement of the $\Delta I = 1/2$ amplitude with respect to the $\Delta I = 3/2$ amplitude. To wit, for the best fits (next favorable minimum) we find

$$\left| \frac{a_{\Delta I=1/2}}{a_{\Delta I=3/2}} \right| = 1.04 (1.05). \quad (17)$$

There is little enhancement of the reduced matrix element corresponding to the tree-level doublet Hamiltonian, $Q_{\pi b}$, with respect to the tree-level quadruplet U . However, the large enhancement of the penguin doublet reduced matrix element $Q_{\pi a}$ over U is analogous to that in the $K \rightarrow \pi\pi$ decays, which has identical isospin analysis to the $B \rightarrow \pi\pi$ case. That a similar enhancement exists in the B system—both in $K\pi$ and $\pi\pi$ final states—is striking, and cries out for a dynamical explanation of the role of flavor symmetries in these enhancements.

C. $B \rightarrow K\bar{K}$

At leading order, decays of B mesons to kaons proceed via the $\Delta S = 0$ Hamiltonian in (12). The K (\bar{K}) transforms as a $\mathbf{2}$ ($\bar{\mathbf{2}}$) under isospin, so the final states decompose under isospin as $\mathbf{2} \times \bar{\mathbf{2}} = \mathbf{1} + \mathbf{3}$.

The reduced matrix elements are then $\langle \mathbf{1} | \mathbf{2}^{(l)} | B \rangle$, $\langle \mathbf{3} | \mathbf{2}^{(l)} | B \rangle$ and $\langle \mathbf{3} | \mathbf{4} | B \rangle$, giving nine parameters to accommodate the seven data entries listed in Table III. Even with a measurement of C and S in $B^0 \rightarrow K^+K^-$ in hand the matrix elements could not be determined unambiguously, but with precise KK data it may be possible to distinguish the physical solution from others.

III. SHORT DISTANCE QCD EFFECTS

How much of the enhancement in the lower dimensional isospin representation matrix elements can be attributed to computable short distance QCD effects? Comparing the effective Hamiltonian in Eq. (2) against the decay amplitudes in Eq. (6), we see that

$$\begin{aligned} \frac{\alpha_s}{8\pi} P_a &= \langle K\pi | \sum_{i=3}^6 C_i(m_b) Q_i | B \rangle \\ &= |C_6(m_b)| \langle \mathbf{2} | \mathbf{1}' | \mathbf{2} \rangle. \end{aligned} \quad (18)$$

Our analysis cannot yield information about the matrix elements of each of the operators $Q_{3,\dots,6}$. The last step in (18) defines the matrix element of the sum of the operators, $\langle \mathbf{2} | \mathbf{1}' | \mathbf{2} \rangle$, after extracting the magnitude of the largest Wilson coefficient, $|C_6|$.

Mode	\mathcal{B} (10^{-6})	A_{CP}	C_f	S_f
$B^+ \rightarrow K^+ \bar{K}^0$	1.19 ± 0.18	0.04 ± 0.14	–	–
$B^0 \rightarrow K^+ K^-$	0.13 ± 0.05	–	–	–
$B^0 \rightarrow K^0 \bar{K}^0$	1.21 ± 0.16	-0.6 ± 0.7	0.0 ± 0.4	-0.8 ± 0.5

TABLE III: Data available in $B \rightarrow K \bar{K}$ decays [22].

Similarly we can define

$$\begin{aligned}
P_b &= \langle K\pi | \sum_{i=1,2} C_i(m_b) Q_i | B \rangle = C_-(m_b) \langle \mathbf{2} | \mathbf{1} | \mathbf{2} \rangle, \\
T &= \langle K\pi | \sum_{i=1,2} C_i(m_b) Q_- | B \rangle = C_-(m_b) \langle \mathbf{2} | \mathbf{3} | \mathbf{2} \rangle, \\
S &= \langle K\pi | \sum_{i=1,2} C_i(m_b) Q_- | B \rangle = C_-(m_b) \langle \mathbf{4} | \mathbf{3} | \mathbf{2} \rangle,
\end{aligned} \tag{19}$$

where $C_\pm = C_1 \pm C_2$ and $Q_\pm = Q_1 \pm Q_2$. The Q_\pm operators do not have definite isospin. However, for the $B \rightarrow \pi\pi$ case the corresponding operator Q_- is pure $\Delta I = 1/2$, so using the Q_\pm basis is natural. Moreover, at 1-loop the operators Q_\pm do not mix among themselves. Hence, to estimate the matrix elements of the “tree” operators we have extracted the coefficient C_- . In any case, since C_\pm are of order 1, this introduces little bias in our analysis.

For our analysis we take the numerical value of Wilson coefficients at NLO in the NDR scheme for $\Lambda_{MS}^{(5)} = 225$ MeV from table 8 of [20]. We find that, for matrix elements from our best fit,

$$\begin{aligned}
|\langle \mathbf{2} | \mathbf{1}' | \mathbf{2} \rangle| &\approx 0.028 \text{ MeV}, & |\langle \mathbf{2} | \mathbf{3} | \mathbf{2} \rangle| &\approx 0.007 \text{ MeV}, \\
|\langle \mathbf{2} | \mathbf{1} | \mathbf{2} \rangle| &\approx 0.006 \text{ MeV}, & |\langle \mathbf{4} | \mathbf{3} | \mathbf{2} \rangle| &\approx 0.002 \text{ MeV}.
\end{aligned} \tag{20}$$

while for the secondary χ^2 minimum

$$\begin{aligned}
|\langle \mathbf{2} | \mathbf{1}' | \mathbf{2} \rangle| &\approx 0.009 \text{ MeV}, & |\langle \mathbf{2} | \mathbf{3} | \mathbf{2} \rangle| &\approx 0.006 \text{ MeV}, \\
|\langle \mathbf{2} | \mathbf{1} | \mathbf{2} \rangle| &\approx 0.041 \text{ MeV}, & |\langle \mathbf{4} | \mathbf{3} | \mathbf{2} \rangle| &\approx 0.002 \text{ MeV}.
\end{aligned} \tag{21}$$

The $\Delta I = 0$ enhancement for both of these sets of matrix elements, Eqs. (10) and (11), corresponds to an enhancement of one or the other

singlet matrix element relative to the largest triplet by a factor of between 4 and 7.

An analogous analysis can be performed for $B \rightarrow \pi\pi$ decays. We define

$$\begin{aligned}
\frac{\alpha_s}{8\pi} Q_{\pi a} &= \langle \pi\pi | \sum_{i=3}^6 C_i(m_b) Q_i | B \rangle \\
&= |C_6(m_b)| \langle \mathbf{1} | \mathbf{2}' | \mathbf{2} \rangle, \\
Q_{\pi b} &= \langle \pi\pi | \sum_{i=1,2} C_i(m_b) Q_i | B \rangle = C_-(m_b) \langle \mathbf{1} | \mathbf{2} | \mathbf{2} \rangle, \\
U &= \langle \pi\pi | C_+(m_b) Q_+ | B \rangle = C_+(m_b) \langle \mathbf{5} | \mathbf{4} | \mathbf{2} \rangle,
\end{aligned} \tag{22}$$

The matrix element of the operator Q_+ can be determined because it is the only “tree” contribution to a $\Delta I = 3/2$ transition. We find that, for matrix elements from our best fit,

$$\begin{aligned}
|\langle \mathbf{1} | \mathbf{2}' | \mathbf{2} \rangle| &\approx 0.040 \text{ MeV}, & |\langle \mathbf{1} | \mathbf{2} | \mathbf{2} \rangle| &\approx 0.007 \text{ MeV}, \\
|\langle \mathbf{5} | \mathbf{4} | \mathbf{2} \rangle| &\approx 0.006 \text{ MeV},
\end{aligned} \tag{23}$$

while for the secondary χ^2 minimum

$$\begin{aligned}
|\langle \mathbf{1} | \mathbf{2}' | \mathbf{2} \rangle| &\approx 0.094 \text{ MeV}, & |\langle \mathbf{1} | \mathbf{2} | \mathbf{2} \rangle| &\approx 0.003 \text{ MeV}, \\
|\langle \mathbf{5} | \mathbf{4} | \mathbf{2} \rangle| &\approx 0.006 \text{ MeV}.
\end{aligned} \tag{24}$$

IV. DISCUSSION AND CONCLUSIONS

There is a striking consistency in the reduced matrix element enhancement that persists in the B decay channels studied. As suggested at the end of Section II B, this may be indicative of the importance of flavor symmetries in non-perturbative regimes in QCD, or perhaps in

new physics contributions (note we have only assumed the quark model, CKM parametrization, *etc.* of the Standard Model). The enhancement of matrix elements with effective Hamiltonians in lower-dimensional isospin representations is only present when penguin diagrams can compete against tree level weak exchanges, which are also the processes where CP violation is predicted at lowest order. These are the $B \rightarrow K\pi$ and $B \rightarrow \pi\pi$ channels in this work.

In our estimates for hadronic matrix elements in Eqs. (20), (23) and (24), but not (21), it is the penguin contributions to the lowest isospin change operator ($\Delta I = 0$ for $B \rightarrow K\pi$ and $\Delta I = 1/2$ for $B \rightarrow \pi\pi$), rather than both penguin and tree contributions, that are enhanced. While we cannot select among the fits *a priori*, in the best fits for both $B \rightarrow K\pi$ and $B \rightarrow \pi\pi$ the penguin dominates the total enhancement, giving a factor of between 4 and 7. The precise value of the enhancement is immaterial: we have made plausible assumptions to remove the short distance QCD effects, but we don't have the means to do this precisely and unambiguously. Moreover, the matrix elements P_a, \dots, U are defined with convenient factors of $\sqrt{2}$ and $\sqrt{3}$ which further adds to the ambiguity. But the enhancement of *amplitudes*, Eqs. (10) (or (11)), is unambiguous. Comparable enhancements in the penguin matrix elements for $B \rightarrow K\pi$ and $B \rightarrow \pi\pi$ lead to a significant amplitude enhancement in $B \rightarrow K\pi$ but very little enhancement in $B \rightarrow \pi\pi$, but only because the latter is CKM-suppressed relative to the former.

ACKNOWLEDGMENTS

DP would like to thank Riccardo Barbieri for valuable discussions. This work was supported in part by the US Department of Energy under contract DE-SC0009919. DP is supported in part by MIUR-FIRB grant RBFR12H1MW. The research of PU has been supported by DOE grant FG02-84-ER40153.

Appendix A: Relevant Observables in B Decays

Here we review the definition of various decay observables employed in our analysis. We will follow the convention of Ref. [22]. We denote an amplitude for the B -meson, B , decaying to final state f by \mathcal{A}_f . The CP-conjugated decay is denoted by $\bar{\mathcal{A}}_{\bar{f}}$. Since we are interested in the s -wave 2-body decay of the B , the partial decay width is given by

$$\Gamma_f = \frac{1}{8\pi} \frac{p_*}{m_B^2} |\mathcal{A}_f|^2 \quad (\text{A1})$$

where p_* is the magnitude of the 3-momentum of one of the daughter particles. The branching ratio, \mathcal{B} , can then be computed from the above partial width.

We are also interested in the CP-violating properties of the decays. For decays of charged B s we can define the direct CP-violation as

$$A_{CP} \equiv \frac{|\bar{\mathcal{A}}_{\bar{f}}|^2 - |\mathcal{A}_f|^2}{|\bar{\mathcal{A}}_{\bar{f}}|^2 + |\mathcal{A}_f|^2}. \quad (\text{A2})$$

In the case of the neutral B^0 decay where the final state f is common to both B^0 and \bar{B}^0 decays, we have to take into account $B^0 - \bar{B}^0$ mixing in defining CP-violating parameters. This occurs when f is a CP eigenstate, *i.e.* $\bar{f} = \pm f$. The two CP-violating parameters can be defined as [25]

$$C_f \equiv \frac{1 - |\lambda_f|^2}{1 + |\lambda_f|^2}, \quad S_f \equiv \frac{2\text{Im}(\lambda_f)}{1 + |\lambda_f|^2}, \quad (\text{A3})$$

where

$$\lambda_f = \frac{V_{tb}^* V_{td} \bar{\mathcal{A}}_f}{V_{tb} V_{td}^* \mathcal{A}_f}. \quad (\text{A4})$$

In case of $B^0 \rightarrow K^0 \pi^0$ decay, neutral kaon mixing contributes an extra factor of $-V_{cd}^* V_{cs} / V_{cd} V_{cs}^*$ in the definition of λ_f .

-
- [1] W. A. Bardeen, A. Buras, and J. Gerard, *Phys.Lett.* **B180**, 133 (1986).
- [2] W. A. Bardeen, A. Buras, and J. Gerard, *Nucl.Phys.* **B293**, 787 (1987).
- [3] W. A. Bardeen, A. Buras, and J. Gerard, *Phys.Lett.* **B192**, 138 (1987).
- [4] A. J. Buras, J.-M. Gerard, and W. A. Bardeen, (2014), [arXiv:1401.1385 \[hep-ph\]](#).
- [5] R. S. Chivukula, J. Flynn, and H. Georgi, *Phys.Lett.* **B171**, 453 (1986).
- [6] T. Blum, P. Boyle, N. Christ, N. Garron, E. Goode, *et al.*, *Phys.Rev.Lett.* **108**, 141601 (2012), [arXiv:1111.1699 \[hep-lat\]](#).
- [7] N. Carrasco, V. Lubicz, and L. Silvestrini, (2013), [arXiv:1312.6691 \[hep-lat\]](#).
- [8] P. Boyle *et al.* (RBC Collaboration, UKQCD Collaboration), *Phys.Rev.Lett.* **110**, 152001 (2013), [arXiv:1212.1474 \[hep-lat\]](#).
- [9] C. Quigg, *Z.Phys.* **C4**, 55 (1980).
- [10] M. Golden and B. Grinstein, *Phys.Lett.* **B222**, 501 (1989).
- [11] T. Aaltonen *et al.* (CDF Collaboration), *Phys.Rev.* **D85**, 012009 (2012), [arXiv:1111.5023 \[hep-ex\]](#).
- [12] T. Aaltonen *et al.* (CDF Collaboration), *Phys.Rev.Lett.* **109**, 111801 (2012), [arXiv:1207.2158 \[hep-ex\]](#).
- [13] R. Aaij *et al.* (LHCb collaboration), (2013), [arXiv:1310.4740 \[hep-ex\]](#).
- [14] D. Pirtskhalava and P. Uttayarat, *Phys.Lett.* **B712**, 81 (2012), [arXiv:1112.5451 \[hep-ph\]](#).
- [15] B. Bhattacharya, M. Gronau, and J. L. Rosner, *Phys.Rev.* **D85**, 054014 (2012), [arXiv:1201.2351 \[hep-ph\]](#).
- [16] T. Feldmann, S. Nandi, and A. Soni, *JHEP* **1206**, 007 (2012), [arXiv:1202.3795 \[hep-ph\]](#).
- [17] J. Brod, Y. Grossman, A. L. Kagan, and J. Zupan, *JHEP* **1210**, 161 (2012), [arXiv:1203.6659 \[hep-ph\]](#).
- [18] H.-Y. Cheng and C.-W. Chiang, *Phys.Rev.* **D86**, 014014 (2012), [arXiv:1205.0580 \[hep-ph\]](#).
- [19] G. Hiller, M. Jung, and S. Schacht, *Phys.Rev.* **D87**, 014024 (2013), [arXiv:1211.3734 \[hep-ph\]](#).
- [20] A. J. Buras, (1998), [arXiv:hep-ph/9806471 \[hep-ph\]](#).
- [21] G. Buchalla, A. J. Buras, and M. E. Lautenbacher, *Rev.Mod.Phys.* **68**, 1125 (1996), [arXiv:hep-ph/9512380 \[hep-ph\]](#).
- [22] J. Beringer *et al.* (Particle Data Group), *Phys.Rev.* **D86**, 010001 (2012).
- [23] L.-L. Chau, H.-Y. Cheng, W. Sze, H. Yao, and B. Tseng, *Phys.Rev.* **D43**, 2176 (1991).
- [24] M. Gronau, J. L. Rosner, and D. London, *Phys.Rev.Lett.* **73**, 21 (1994), [arXiv:hep-ph/9404282 \[hep-ph\]](#).
- [25] Here we ignore the effect of CP-violation in $B^0 - \bar{B}^0$ mixing which is less than 1%.